Available online at www.sciencedirect.com
ScienceDirect
Journal of Solid State Chemistry 179 (2006) 2827–2833
JOURNAL OF SOLID STATE CHEMISTRY
www.elsevier.com/locate/jssc

Stability of lithium in α-rhombohedral boron

Wataru Hayami*, Takaho Tanaka, Shigeki Otani

Advanced Materials Laboratory, National Institute for Materials Science, 1-1 Namiki, Tsukuba, Ibaraki 305-0044, Japan

Received 19 August 2005; received in revised form 22 October 2005; accepted 16 January 2006
Available online 14 February 2006

Abstract

The stability of lithium atoms in α-rhombohedral boron was studied by the density functional theory and Car–Parrinello molecular dynamics (MD) simulations. At a low Li concentration (1.03 at%), a Li atom at the center of the icosahedral B_{12} site (the *I*-site) was found to be metastable, and the potential barrier was estimated at 775 ± 25 K ($= 67 \pm 25$ meV). Over 800 K, Li atoms began to escape from the B_{12} cage and settled at the tetrahedral site (the *T*-site) or at the octahedral site (the *O*-site). Li at the *T*-site was also metastable below 1400 K, and Li at the *O*-site was energetically the most favorable. At a high Li concentration (7.69 at%), the *I*-site changed to an unstable saddle point. The *T*-site was still metastable, and the *O*-site was the most stable. Regardless of concentration, MD simulations showed that Li atoms at the *O*-site never jumped to other sites below 1400 K. The migration of Li would be very slow below this temperature.

Keywords: Boron; Lithium; Density functional theory; Molecular dynamics simulation

1. Introduction

Boron atoms form a variety of structures through covalent bonds [1]. It is well known that elemental boron and boron-rich compounds have a characteristic icosahedral structure comprised of 12 atoms. Icosahedral structures with 13 atoms are often observed in metallic clusters because 13 atoms can favorably form a close-packed structure. However, in the case of B_{12}, there is a vacancy at the center. This unique structure has attracted a great deal of attention in the form of both experimental and theoretical studies.

α-Rhombohedral (α-rh) boron has one B_{12} icosahedron per unit cell (Fig. 1). This structure was first determined by Decker and Kasper [2], and later refined by Morosin et al. [3] and Will and Kiefer [4]. Theoretical studies on α-rh boron and related compounds like $B_{12}P_2$, $B_{12}As_2$, $B_{12}O_2$, and $B_{12}C_3$ have been reported [7–25]. Intercalated atoms, P, As, and O, are on the diagonal axis around the center of the unit cell [3,5,6]. Theoretical studies of B_{12} and other boron clusters have also been conducted [26–33].

Intercalation into the center of a B_{12} icosahedron has yet to be observed in any boron compound, which suggests that it is not easy to thermally dope an atom into the icosahedron. If this doping can be achieved, numerous new materials with *X* at B_{12} (an *X* atom in a B_{12} icosahedron) structural units could be composed. Therefore, it is important to study the stabilities of B_{12} and *X* at B_{12} icosahedra.

A theoretical study by Kawai and Weare [26] showed that the B_{13} icosahedron is not stable. Another first-principles calculation by Gunji and Kamimura [14] showed that Li at B_{12} (a Li atom in the B_{12} cage) is energetically unstable with α-rh boron, but that Li at Li_3B_{12} (a Li atom in the B_{12} cage and three Li atoms in the intercalation sites) is stable. In theoretical work by Hayami [30], calculations using cluster models AB_{12} (A = H–Ne) suggested that H and Li atoms could occupy the B_{12} cage. Experimentally, Soga et al. [34] and Terauchi et al. [35] produced a Li- and Mg-doped α- and β-rh boron and examined its atomic and electronic properties. In the case of the Li-doped α-rh boron, they observed a slight increase in the density of states at the Fermi level by electron energy loss spectroscopy (EELS). Comparing the EELS spectra and the calculated density of states in previous work [14], the

*Corresponding author. Fax: +81 29 852 7449.
E-mail address: hayami.wataru@nims.go.jp (W. Hayami).

0022-4596/$ - see front matter © 2006 Elsevier Inc. All rights reserved.
doi:10.1016/j.jssc.2006.01.026

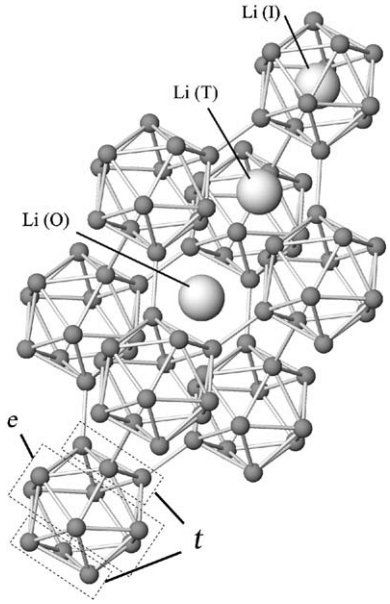

Fig. 1. Structure of α-rhombohedral boron. Boron atoms (small spheres) form icosahedra, and the icosahedra form a rhombohedral lattice. Large spheres indicate three possible Li sites, icosahedral (*I*-), tetrahedral (*T*-), and octahedral (*O*-), from top to bottom. The B atoms in an icosahedron are classified into two groups: six B atoms, denoted by "*t*", that make bonds with neighboring icosahedra, and the other six B atoms denoted by "*e*". This notation was adopted from Ref. [9].

number of Li atoms was found to be small, indicating Li was probably not in the B_{12} cage but rather in the intercalation sites. The precise location of Li was unknown since the X-ray diffraction pattern exhibited little change with the Li doping. In the former calculations [14,30], the concentration of Li to boron was rather large; at least one Li to each B_{12} icosahedron, and it is not known if Li at B_{12} is stable or not at low Li concentrations, which would likely represent the practical cases.

We chose lithium because it is a promising candidate according to our previous study [30], and the experimental data to compare are available [34,35]. First-principles calculations using a large unit cell ($B_{96} = (B_{12})_8$) with Li as the dopant were performed to investigate the stability of Li at B_{12}. The total energies of the optimized structures were calculated by the density functional theory, followed by molecular dynamics (MD) simulations at finite temperatures. The stabilities of Li at the other sites were also investigated to compare with the experimental data.

2. Computational details

The calculations of the total energies and the Car–Parrinello MD [36] were performed using the CPMD code version 3.9.1 [37,38]. This code is based on the density functional theory [39,40] with plane waves and pseudopotentials. The norm-conserving, Troullier–Martins-type pseudopotentials [41] were used. The generalized gradient approximation was included with the functional derived by Becke [42] and Lee et al. [43]. An energy cutoff of 40 Ry was enough to provide a convergence of the total energy. Since the unit cell is large, *k*-point sampling in the total-energy calculation was done using Monkhorst–Pack sampling [44] of a $(2 \times 2 \times 2)$ mesh. The results were compared with those of a finer mesh, and it was found that the difference in the total energy per atom was less than 6×10^{-4} eV. For the MD, the calculations were performed at the Γ point. We performed some MD simulations with a finer $(2 \times 2 \times 2)$ mesh and obtained almost the same structures. The temperature was controlled by scaling the total kinetic energy (KE) of the atoms at every time step. The time step was 5.0 a.u. (0.121 fs).

3. Results and discussion

A unit cell of α-rh boron consists of a B_{12} icosahedron and the icosahedra stack as in an fcc structure along the $\langle 1\,1\,1 \rangle$ direction (Fig. 1). Experimental data for the lattice parameters are $a = 5.0643$ Å and $\alpha = 58.0962^\circ$ ($\alpha = 60^\circ$ in an ideal fcc structure) [3]. In our computational model, a $2 \times 2 \times 2$ unit cell comprised of $(B_{12})_8 = B_{96}$ atoms was used. The large spheres in Fig. 1 indicate three possible Li sites, icosahedral (*I*-), tetrahedral (*T*-), and octahedral (*O*-) from top to bottom. The *T*-site is the center of four B_{12} clusters and the *O*-site is the center of the $\langle 1\,1\,1 \rangle$ diagonal axis of the unit cell. Our unit cell has eight *I*- and *O*-sites, and 16 *T*-sites, so that the number of Li atoms is variable from 1 to 8 at the *I*- and *O*-sites and from 1 to 16 at the *T*-sites.

First, one Li atom was placed at the *I*-site and the whole structure including lattice parameters was optimized. Only the rhombohedral symmetry of the lattice was assumed, and the geometry of atoms was optimized without any constraints. The concentration of Li was about 1.03 at% in this case, which is much smaller than in previous studies [14,30]. When the geometry was fully optimized, Li still remained at the *I*-site. However, the binding energy, defined here as $E(B_{96}) + E(\mathrm{Li}) - E(\mathrm{LiB}_{96})$, where E is the total energy, was -4.99 eV. Since the binding energy is negative, the *I*-site for Li is not globally stable, but instead is metastable, or a saddle point. The definition of stability in this work is given as follows:

Stable: The total energy of a system (Li–B) is at the global minimum.
Metastable: The total energy of a system is at a local minimum but not at the global minimum.
Unstable: The total energy of a system is neither at the global minimum nor at a local minimum.

It should be noted that the binding energy must be positive to be a global minimum.

Since the total energy can be calculated accurately enough, the problem is to determine if the system is at a local (or global) minimum or not. In total-energy calculations, the geometry of atoms is always optimized, so that one may think the system is already at a local or the global

minimum. This is not true, however, because the system may be at a 'saddle point' where the total energy is at a minimum along a certain direction of the atomic coordinates but at a maximum along another direction. To check this, the total energies must be calculated with each atomic coordinate slightly shifted, which is a laborious task when many atoms are concerned as in our case.

Instead of doing this, we employed the Car–Parrinello MD simulation. The advantages of the MD simulation are that (1) it effectively surveys the coordinates space, and (2) it can estimate the potential barrier when the system is at a local or the global minimum. When the starting geometry is already optimized, it requires rather a short time to determine whether the system is at a saddle point, because if so, the structure immediately deviates from the equilibrium point. The change occurs typically in ~100 fs at room temperature.

Fig. 2 shows the trajectories of Li and the surrounding B atoms projected onto a plane normal to the $\langle 1\,1\,1\rangle$ direction. Only six *e*-borons (see Fig. 1) are plotted. At 300 K, the Li and boron atoms oscillate in the localized area keeping the icosahedral structure unchanged. Therefore, the *I*-site for Li is not a saddle point but a metastable site. At a temperature around 700–750 K, the icosahedron begins to deform. In Fig. 2(b) and (c), the bottom and the right bottom B are moving separately, and at 800 K, Li finally escapes from the B_{12} cage and B_{12} returns to an icosahedron. The escape temperature is estimated to be 775 ± 25 K, corresponding to a potential barrier of 67 ± 2.2 meV. This value is much smaller than the absolute value of the binding energy. After moving out of the cage, the Li atom settled at the *O*-site at 800 K, but it settled at the *T*-site in a simulation at 1200 K. The potential barrier to the *O*-site may be a little lower than that to the *I*-site, but more MD simulations are required to make a statistically meaningful estimation.

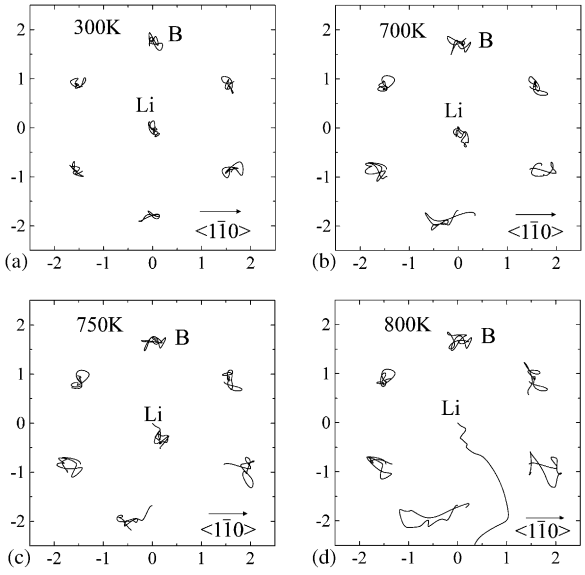

Fig. 2. Trajectories of Li atoms at the *I*-site and the surrounding six *e*-B atoms. The projection plane is normal to the $\langle 1\,1\,1\rangle$ direction. The unit of scale is angstroms. The time step is 0.121 fs, and the number of steps is 2000 (241.8 fs). (a) $T=300$ K, (b) $T=700$ K, (c) $T=750$ K, and (d) $T=800$ K. Li escapes out of the B_{12} cage.

The estimation of the potential barrier by MD simulation must be carefully done with consideration of statistical mechanics. In real systems, the motion of atoms obeys the Maxwell–Boltzmann distribution. The average of the KE of an atom is $3/2kT$ (k is the Boltzmann constant) and the standard deviation is also about kT. Since the potential barrier for a Li atom is determined not only by the Li but also the surrounding B atoms, the sum of the KE of Li and B atoms should be taken into account. When the KE exceeds a certain value, a Li atom can move to another site and then the KE is regarded as equal to the potential barrier. When the standard deviation of the KE of an atom is σ, the central limit theorem tells us the standard deviation of the KE of N atoms becomes $\sigma/\sqrt{N}$). Assuming the number of Li and surrounding B atoms is about 5–20, the standard deviation is $\sigma/2.2$–$\sigma/4.5$. When the temperature is 800 K, e.g., it corresponds to about 180–360 K, and it is impossible to estimate the potential barrier correctly by a single MD simulation.

To avoid this problem, as described in Section 2, the sum of KE in the unit cell is normalized to $3/2NkT$ at every step, where N is the number of atoms in the unit cell. Then, compared with the real system, the fluctuation of the KE is extremely suppressed because the Maxwell–Boltzmann distribution turns into a distribution like $f=\exp[-(1/kT)(E+E^2/2cT+\cdots)]$, where E is the total energy of the system and c the heat capacity of the heat reservoir. The E^2 term cannot be neglected and it works to suppress the fluctuation. This change occurs because the atoms in the unit cell work as a heat reservoir by themselves and the number of atoms are limited (about 100 atoms in our case). A very large heat reservoir is required to hold the Maxwell–Boltzmann distribution. When the fluctuation of KE is small enough, if the sum of KE of Li and surrounding B atoms is smaller than the potential barrier, the Li atom is expected to keep staying at the site for a long time, and once the sum of KE exceeds the potential barrier, the Li atoms immediately moves to another site. Consequently, a single and short-time MD simulation can provide a good estimation of the potential barrier. To confirm if the fluctuation of KE is actually small, we performed a long-time MD simulation with a Li atom at the *I*-site in LiB_{96}. The time length was 2.41 ps, and the temperature was set to the same as in Fig. 2(c), 750 K. The time is 10 times longer than in Fig. 2. It was observed that the Li atom kept staying at the site even at this temperature. Another evidence for the small fluctuation is Fig. 2(d), where the Li atom seems to move out very quickly. Therefore, it is certain that the fluctuation of KE is small enough under the present condition. It should be remembered that MD simulations in this work are for the estimation of potential barriers but not for the simulation of real systems.

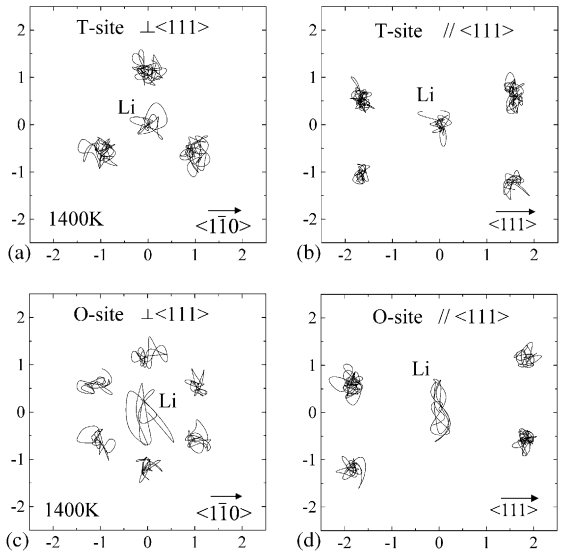

Fig. 3. Trajectories of Li at the *T*- and *O*-sites. The temperature is 1400 K. The unit of scale is angstroms. The time step is 0.121 fs, and the number of steps is 4000 (483.8 fs). The projection plane is normal to the ⟨1 1 1⟩ direction for (a) and (c), and parallel for (b) and (d). (a) and (b) a Li atom at the *T*-site and six neighboring B atoms. (c) and (d) a Li atom at the *O*-site and six neighboring B atoms.

Next, a Li atom was placed at the *T*- and *O*-sites and the total energies were calculated after optimizing the geometries. In both cases, Li stayed at each site. The binding energies for Li are −1.04 eV (*T*-site) and +0.17 eV (*O*-site). Therefore, only the *O*-site is energetically stable. These results cannot be compared directly with the results by Gunji and Kamimura [14] because of differences in the Li concentration, but both results exhibited a similar tendency in that the *O*-site was the most stable and the *I*-site produced a negative binding energy for Li. As in the case of the *I*-site, MD simulations were performed for both the *T*- and *O*-sites.

Fig. 3 shows the projected trajectories at 1400 K. (a) and (c) are on the planes normal to the ⟨1 1 1⟩ direction, and (b) and (d) are parallel to the ⟨1 1 1⟩ direction. At the *T*-site (Fig. 3(a) and (b)), Li moves in a relatively localized area, with the distribution of the trajectory being almost isotropic. At the *O*-site, the Li trajectory was spread over a wider area on the plane normal to the ⟨1 1 1⟩ direction (Fig. 3(c)), but not to the ⟨1 1 1⟩ direction (Fig. 3(d)). This indicates that the potential for Li is not isotropic. For both the *T*- and *O*-sites, Li does not migrate out of the sites at this temperature, which means that the *T*-site is metastable and the *O*-site is stable.

The binding energies, potential barriers, and Li–B distances for Li are summarized in Table 1. The potential barrier between the *T*- and *O*-sites is over 1400 K. An MD simulation at a higher temperature is meaningless for the present purposes because the phase transition to *β*-rh boron occurs at 1400 K [45]. For compounds like boron phosphide $B_{12}P_2$, P is located between the *T*- and *O*-sites [3,5,6], but no metastable points for a single Li were

Table 1
Binding energies, potential barriers, and Li–B distances for Li in LiB_{96}

	Binding energy (eV)	Potential barrier (eV)	Li–B distance (Å)
I-site	−4.99	0.067 (775 K)	1.76
T-site	−1.04	>0.12 (1400 K)	1.91
O-site	0.17	Stable	2.18

Only the *O*-site is energetically stable, while the other two sites are metastable. The potential barrier between the *T*- and *O*-sites is not exactly known (more than 1400 K = 0.12 eV).

observed at these locations in this study. It seems reasonable that the distances between Li and B are aligned in the same order as the binding energies. They are smaller than the sum of each atomic radius, 1.52 Å (Li) and 0.795 Å (B), which partly explains why the binding energies are so small in this system.

With respect to the binding energy, only the *O*-site has a positive value such that Li could be thermally doped into this site. However, considering the potential barrier to neighboring sites, it is likely that the diffusion coefficient of Li is very small below 1400 K. This explains why Li was doped only in a small part of the sample [34,35], and the amount of Li is small even in the doped areas. Thermal doping may be facilitated through defects or grain boundaries.

The bond lengths of α-rh boron with a Li atom at the *I*-site are listed in Table 2. The calculated bond lengths of pure boron (a) are in good agreement with the experimental values (d) [3,4] and the previous report [9]. Compared with the experiment, the calculated error is less than 1.2% for intra-icosahedron (intra) bonds and the *t*–*t* bonds in inter-icosahedron (inter). For the inter *e*–*e* bonds, the error is a little larger (2.2%). It is well known that the inter *t*–*t* bond is shorter than the intra *t*–*t* bond. When a Li atom is put at one of the *I*-sites, the total icosahedron deforms (b). The regular triangle composed of intra *t*–*t*–*t* bonds transforms to an isosceles triangle. The intra *t*–*t* bond expands by 2.3–4.6%, the intra *t*–*e* bond by 2.8–7.9%, and the intra *e*–*e* bond by 3.4–6.8%. The expansion rate for *t*–*t* is a little smaller than the other two, which would reflect the strength of these bonds. Interestingly, Li always leaves the B_{12} cage through the *e*-borons. On the other hand, the inter *t*–*t* and *e*–*e* bonds contract by 2.4% and 2.9–4.9%, respectively. Since the expansion of the icosahedron is made possible by these inter-bond contractions, additional Li atoms at the *I*-sites may weaken the icosahedra. The bond lengths of B_{12} without Li do not change as much (c).

Two and four Li atoms were put at the *I*-sites to examine the concentration dependence of the stability. For the distribution of Li atoms among eight *I*-sites, there are three cases for two Li atoms, and 13 cases for four Li atoms. Since it is not efficient to check all the cases, we selected three cases as shown in Fig. 4. In two cases (Fig. 4(a)), Li atoms escaped from the B_{12} cage at about 275 ± 25 K. The

Table 2
Bond lengths of α-rh boron with a Li atom at the *I*-site

		Intra-icosahedron (Å)			Inter-icosahedron (Å)	
		t–t	*t–e*	*e–e*	*t–t*	*e–e*
(a)	$(B_{12})_8$	1.75	1.78	1.77	1.68	2.06
(b)	$Li(B_{12})_8$ (*I*-site)	1.79–1.83	1.83–1.92	1.83–1.89	1.64	1.96–2.00
	B_{12} including Li	(2.3–4.6%)	(2.8–7.9%)	(3.4–6.8%)	(−2.4%)	(−4.9−−2.9%)
(c)	$Li(B_{12})_8$ (*I*-site)	1.75	1.769–1.799	1.75–1.77	1.67–1.68	2.044–2.117
	B_{12} without Li					
(d)	Experiment	1.754	1.80	1.784	1.671	2.013

(a) Pure boron (calculated); (b) B_{12} icosahedron including Li. The numbers in parentheses are the expansion rates compared with (a). (c) B_{12} icosahedron without Li; (d) the experimental values taken from Refs. [3,4].

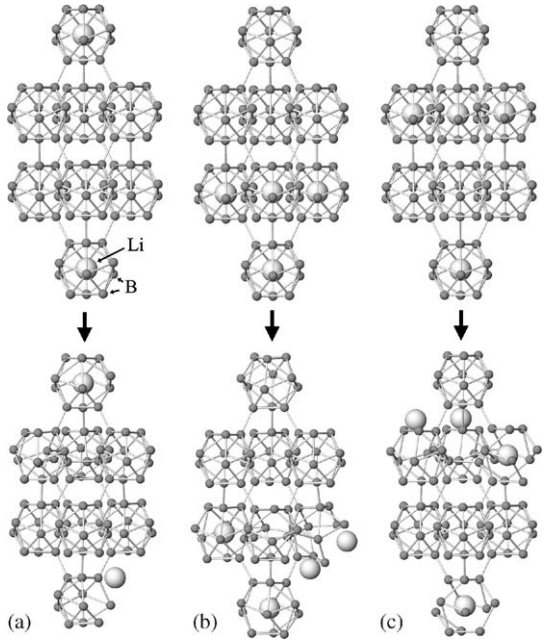

Fig. 4. MD simulations with two and four Li atoms at the *I*-site. (a) Li_2B_{96}: $T = 300$ K. Li atoms escape from B_{12} at 275 ± 25 K. (b) and (c) Li_4B_{96}: $T = 10$ K. Li atoms are almost unstable.

corresponding potential barrier is 24 ± 2.2 meV, which is about one-third of the one Li case. In four cases (Fig. 4(b) and (c)), Li atoms moved out of the B_{12} cage even at 10 K, which suggests the structure is almost unstable. From these results, it seems likely that the stability of Li at the *I*-site is weakened by the increase of its concentration.

To observe the stability of Li at a high concentration, eight Li atoms were put on the *I*-, *T*-, and *O*-sites in the $2 \times 2 \times 2$ cell ($Li_8B_{96} = (LiB_{12})_8$). The concentration of Li was 7.69 at%. The binding energies per Li atom, potential barriers, the optimized lattice parameters, and Li–B distances are listed in Table 3. Here, the binding energy per Li atom is defined as $\{E(B_{96}) + 8E(Li) — E(Li_8B_{96})\}/8$. For all of the sites, the binding energies were only slightly higher (more stable) than in the case of LiB_{96} (Table 1), and the energy differences between the sites were similar. In a previous report [14], the difference between the *I*-site (−2.86 eV) and the *O*-site (2.38 eV) was listed as 5.24 eV, which is close to the result in this study (5.01 eV), but the absolute binding energies are about 2 eV higher than in our results. This discrepancy can probably be attributed to the difference in the method of geometrical optimization, basis functions, and the exchange-correlation functional. The geometry in Ref. [14] was partially optimized using parameters, whereas in our calculation, it was fully optimized. The lattice parameters of Li_8B_{96} expanded by 3.1% for the *I*- and *T*-sites, and by 2.0% for the *O*-site compared with the calculated values for pure boron. The changes in the inter-axis angle α were generally small. The Li–B distances are a little larger than those in LiB_{96}.

MD simulations at finite temperatures were performed to check the stability of Li_8B_{96}. Fig. 5 shows an example of the *I*-site at 10 K. At first, the Li atom remains at the center for a moment ((a)). Once the Li atom shifts from the center, it quickly slips out of the cage ((b)–(d)), and B_{12} returns to an icosahedron. This means that the *I*-site is almost unstable (probably a saddle point). When the Li atom is moving out of the cage, it always breaks the intra *e–e* bonds, which would suggest that the intra *e–e* bonds are weaker than the intra *t–t* bonds.

MD simulations with eight Li atoms at the *T*-site indicated that Li atoms begin to hop to the *O*-site at about 950 K (Fig. 6(a)). The *T*-site is metastable, but not as stable as in the low concentration, in which Li hopping did not occur below 1400 K (Fig. 3). MD simulations with eight Li atoms at the *O*-site indicated that the *O*-site is stable and the potential barrier is larger than 1400 K (Fig. 6(b)). Considering these results, the most stable site for Li is the *O*-site regardless of Li concentration. It is also clear that the thermal diffusion of Li in α-rh boron is obstructed by the high potential barrier.

4. Conclusions

The stability of Li in α-rh boron was investigated by first-principles calculations of the total energies and molecular dynamics simulations. At low concentrations (LiB_{96}), a Li atom at the *I*- and *T*-sites is metastable. The potential barrier for the *I*-site is 775 ± 25 K (67 ± 2.2 meV), and that

Table 3
Binding energies per Li atom, potential barriers, the optimized lattice parameters and Li–B distances of Li_8B_{96}

	Binding energy (eV)	Potential barrier (eV)	Lattice parameter a (Å) α (deg.)		Li–B distance (Å)
I-site	−4.60	~0	5.20	58.1	1.79
T-site	−0.71	0.08(925 K)	5.20	58.4	1.93
O-site	0.41	Stable	5.14	57.7	2.23
B_{96}					
Calculated			5.04	58.6	
Experimental			5.064	58.096	

All three sites have a slightly larger binding energy than in LiB_{96}, with the *O*-site being the most stable. The *I*-site becomes unstable and the potential barrier for the *T*-site is lowered.

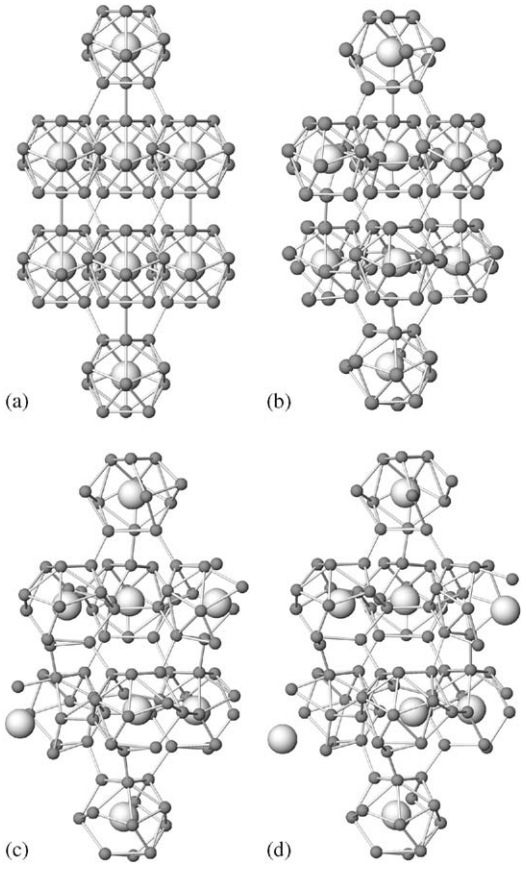

Fig. 5. MD simulations of eight Li at the *I*-site at 10 K. (a) $t = 0$ and (b) $t = 484$ fs. A Li atom at the bottom-left begins to move. (c) $t = 726$ fs. Another Li at the top-right begins to move. (d) $t = 847$ fs. The bottom-left Li moves toward the *O*-site.

for the *T*-site is larger than 1400 K. A Li atom is most stable at the *O*-site. Only the *O*-site has a positive binding energy. The stability of Li at the *I*-site seems to be weakened as the Li concentration increases (Li_2B_{96}, Li_4B_{96}). At high concentrations ($(LiB_{12})_8$), the *I*-site becomes unstable (saddle point) and the *T*-site remains metastable with a potential barrier of 925 ± 25 K (80 ± 2.2 meV). In every case, the *O*-site is the most stable.

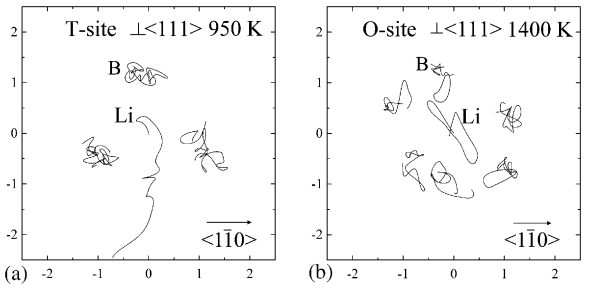

Fig. 6. Trajectories of Li at the (a) *T*-site at 950 K and (b) *O*-site at 1400 K. The unit of scale is angstroms. The time step is 0.121 fs, and the number of steps is 2000 (241.9 fs). The projection plane is normal to the $\langle 1\,1\,1 \rangle$ direction.

Independent of the concentration, Li at the *O*-site does not migrate to the other sites below 1400 K, indicating a small diffusion coefficient, which is in agreement with past experimental results.

Since Li at the *I*-site was proven to be metastable at low concentrations, the Li at B_{12} structure could theoretically form. However, since the total energy of Li at the *I*-site is much higher (5.01–5.16 eV) than that at the *O*-site, and the stabilizing energy is very small (0.067 eV = 775 K), it would not be easy to attain this structure experimentally.

Acknowledgment

We would like to thank Takashi Aizawa for valuable discussions.

References

[1] R.M. Adams, Boron, Metallo-Boron Compounds and Boranes, Interscience Publishers, Wiley, New York, 1964.
[2] B.F. Decker, J.S. Kasper, Acta Crystallogr. 12 (1959) 503.
[3] B. Morosin, A.W. Mullendore, D. Emin, G.A. Slack, AIP Conference Proceedings, vol. 140, American Institute of Physics, New York, 1986, p.70.
[4] G. Will, B.Z. Kiefer, Anorg. Allg. Chem. 627 (2001) 2100.
[5] G.A. Slack, T.F. McNelly, E.A. Taft, J. Phys. Chem. Solids 44 (1983) 1009.
[6] P. Yang, T.L. Aselage, Powder Diffr. 10 (1995) 263.
[7] H.C. Longuet-Higgins, M. deV. Roberts, Proc. R. Soc. Lond. 230A (1955) 110.

[8] D.W. Bullett, J. Phys. C: Solid State Phys. 15 (1982) 415.
[9] S. Lee, D.M. Bylander, L. Kleinman, Phys. Rev. B 42 (1990) 1316.
[10] D.M. Bylander, L. Kleinman, S. Lee, Phys. Rev. B 42 (1990) 1394.
[11] C.L. Beckel, M. Yousaf, M.Z. Fuka, S.Y. Raja, N. Lu, Phys. Rev. B 44 (1991) 2535.
[12] S. Lee, D.M. Bylander, L. Kleinman, Phys. Rev. B 45 (1992) 3245.
[13] S. Gunji, H. Kamimura, T.J. Nakayama, Phys. Soc. Jpn. 62 (1993) 2408.
[14] S. Gunji, H. Kamimura, Phys. Rev. B 54 (1996) 13665.
[15] D. Li, W.Y. Ching, Phys. Rev. B 52 (1995) 17073.
[16] N. Vast, S. Baroni, G. Zerah, J.M. Besson, A. Polian, M. Grimsditch, J.C. Chervin, Phys. Rev. Lett. 78 (1997) 693.
[17] N. Vast, J.M. Besson, S. Baroni, A. Dal Corso, Compt. Mater. Sci. 17 (2000) 127.
[18] K. Shirai, H. Katayama-Yoshida, J. Phys. Soc. Jpn. 67 (1998) 3801; K. Shirai, H. Katayama-Yoshida, Physica B 263–264 (1999) 791.
[19] M. Fujimori, T. Nakata, T. Nakayama, E. Nishibori, K. Kimura, M. Takata, M. Sakata, Phys. Rev. Lett. 82 (1999) 4452.
[20] J. Zhao, J.P. Lu, Phys. Rev. B 66 (2002) 092101.
[21] A. Masago, K. Shirai, H. Katayama-Yoshida, Mol. Simulation 30 (2004) 935.
[22] K. Shirai, A. Masago, H. Katayama-Yoshida, Phys. Stat. Sol. (b) 241 (2004) 3161.
[23] D. Emin, D.G. Evans, S.S. McCready, Phys. Stat. Sol. (b) 205 (1998) 311.
[24] D. Emin, Solid State Chem. 177 (2004) 1619; D. Emin, Phys. Rev. B 61 (2000) 6069; D. Emin, Phys. Rev. B 59 (1999) 6205.
[25] T.L. Aselage, D. Emin, S.S. McCready, Phys. Rev. B 64 (2001) 054302; T.L. Aselage, D. Emin, S.S. McCready, Phys. Stat. Sol. (b) 218 (2000) 255.
[26] R. Kawai, J.H. Weare, Chem. Phys. Lett. 191 (1992) 311.
[27] H. Kato, K. Yamashita, K. Morokuma, Bull. Chem. Soc. Jpn. 66 (1993) 3358.
[28] M. Fujimori, K.J. Kimura, Solid State. Chem. 133 (1997) 178.
[29] F. Gu, X. Yang, A. Tang, H. Jiao, P.J. Schleyer, Comp. Chem. 19 (1998) 203.
[30] W. Hayami, Phys. Rev. B 60 (1999) 1523.
[31] I. Boustani, Chem. Phys. Lett. 240 (1995) 135; I. Boustani, Phys. Rev. B 55 (1997) 16426; I. Boustani, J. Solid State Chem. 133 (1997) 182.
[32] S. Chacko, D.G. Kanhere, I. Boustani, Phys. Rev. B 68 (2003) 035414.
[33] S.J. Xu, J.M. Nilles, D. Radisic, W.J. Zheng, S. Stokes, K.H. Bowen, R.C. Becker, I. Boustani, Chem. Phys. Lett. 379 (2003) 282.
[34] K. Soga, A. Oguri, S. Araake, M. Terauchi, A. Fujiwara, K. Kimura, J. Solid State Chem. 177 (2004) 498.
[35] M. Terauchi, A. Oguri, K. Kimura, A. Fujiwara, J. Electron Microsc. 53 (2004) 589.
[36] R. Car, M. Parrinello, Phys. Rev. Lett. 55 (1985) 2471.
[37] CPMD, Copyright IBM Corp. 1990–2004, Copyright MPI fur Festkorperforschung Stuttgart 1997–2001, 〈http://www.cpmd.org/〉.
[38] D. Marx, J. Hutter, NIC Series, Vol.1, John von Neumann Institute for Computing, Jülich, 2000 (pp. 301–449).
[39] P. Hohenberg, W. Kohn, Phys. Rev. 136 (1964) B864.
[40] W. Kohn, L.J. Sham, Phys. Rev. 140 (1965) A1133.
[41] N. Troullier, J.L. Martins, Phys. Rev. B 43 (1991) 1993.
[42] A.D. Becke, Phys. Rev. A 38 (1988) 3098.
[43] C. Lee, W. Yang, R.G. Parr, Phys. Rev. B 37 (1988) 785.
[44] H.J. Monkhorst, J.D. Pack, Phys. Rev. B 13 (1976) 5188.
[45] P. Runow, J. Mater. Sci. 7 (1972) 499.